# Diattenuation Imaging of Brain Tissue Explored by Finite-Difference Time-Domain Simulations

Presented During: Poster Session
Thursday, June 13, 2019: 12:45 PM - 02:45 PM

#### Poster No:

Th549

# **Submission Type:**

Abstract Submission

#### **Authors:**

Miriam Menzel<sup>1</sup>, Markus Axer<sup>1</sup>, Katrin Amunts<sup>1</sup>, Hans De Raedt<sup>2</sup>, Kristel Michielsen<sup>1</sup>

# Institutions:

<sup>1</sup>Forschungszentrum Jülich GmbH, Jülich, Germany, <sup>2</sup>University of Groningen, Groningen, Netherlands

## Introduction:

Three-dimensional Polarized Light Imaging (3D-PLI) reconstructs the brain's nerve fiber architecture by measuring the birefringence of unstained histological brain sections with micrometer resolution [1,2]. The anisotropy that causes the birefringence (anisotropic refraction) also leads to diattenuation (anisotropic attenuation). In recent work, we have introduced Diattenuation Imaging (DI) – a combined measurement of 3D-PLI and diattenuation, which highlights different brain tissue structures [3]: in some brain regions, the light is minimally attenuated when it is polarized parallel to the nerve fibers (referred to as D+), in others, it is maximally attenuated (referred to as D-). Here, we show with experimental studies and finite-difference time-domain (FDTD) simulations [4] that the diattenuation signal depends not only on the nerve fiber orientation but also on other brain tissue properties like tissue homogeneity, myelin sheath thickness, and fiber size.

# Methods:

The experimental studies were performed on formalin-fixated,  $60\,\mu m$  thick sections of a rat and a vervet monkey brain, embedded in 20 % glycerin solution [4]. The 3D-PLI and diattenuation measurements were performed with the polarimetric set-ups shown in Fig. 1A,D. The phases  $\{\phi_P,\phi_D\}$  of the resulting 3D-PLI and diattenuation signals and the normalized amplitude of the diattenuation signal |D| (see Fig. 1B) were used to generate colored diattenuation images (see middle panel in Fig. 1C): all |D| values belonging to regions with  $\phi_D \approx \phi_P$  ( $\phi_D \approx \phi_P + 90^\circ$ ) were colorized in green (magenta), representing regions with diattenuation of type D+ (D-). The simulation studies were performed for artificial nerve fiber bundles with different out-of-plane inclination angles  $\alpha$  (see Fig. 2B, bottom right) and for a horizontal fiber bundle with different fiber properties, see Fig. 2C. The propagation of the light wave through the sample was computed with TDME3D [4,5], a massively parallel Maxwell Solver based on an unconditionally-stable FDTD algorithm. The refractive indices of axons (1.35), myelin sheaths (1.47), and surrounding medium (1.37) were chosen according to literature values; the multi-layered myelin sheath was modeled by two layers to reduce computing time [4].

OHBM 09.12.2019, 10:39 https://ww5.aieyolution.com/hb...

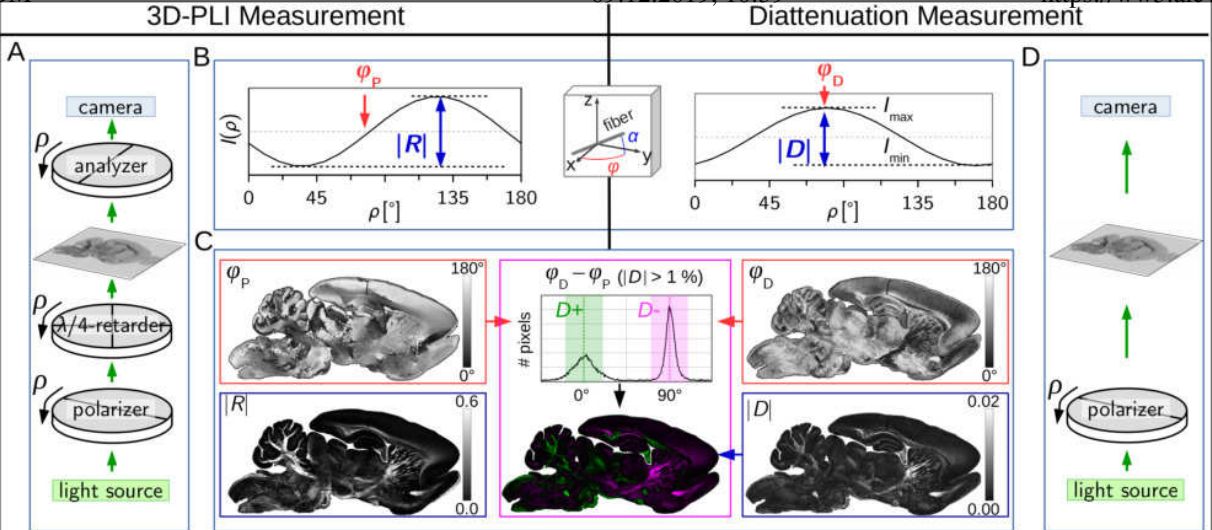
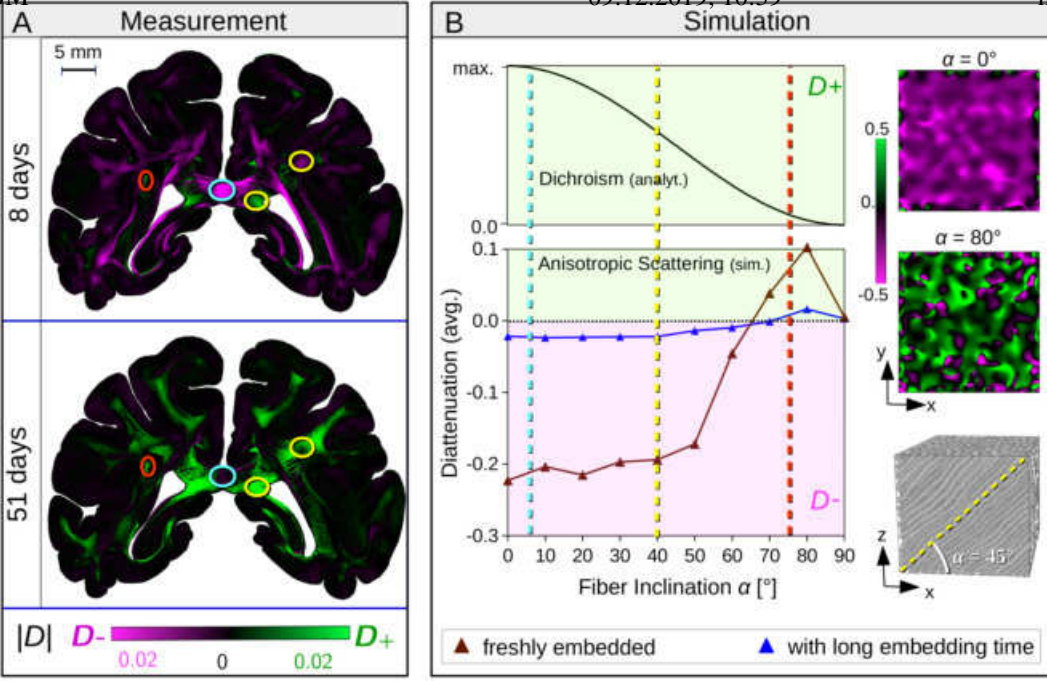


**Figure 1. Diattenuation Imaging:** combined measurement of 3D-PLI (left) and diattenuation (right), shown exemplary for a sagittal rat brain section. (A,D) Measurement set-up consisting of a pair of crossed linear polarizers and a quarter-wave retarder rotated by angles  $\rho = \{0,10,...,170\}^\circ$ . (B) 3D-PLI and diattenuation signals (transmitted light intensities  $I(\rho)$ ). (C) The colored diattenuation image (middle image) is computed from the normalized amplitude of the diattenuation signal |D|, considering the phases  $\{\varphi_p,\varphi_p\}$  of the 3D-PLI and diattenuation signals: all |D| values belonging to regions with  $(\varphi_p - \varphi_p) \in [-20^\circ, 20^\circ]$  are colorized in green (D+), regions with  $(\varphi_p - \varphi_p) \in [-20^\circ, 20^\circ]$  are colorized in magenta (D-), see peaks in histogram. The figure was adapted from Menzel et al. (2018) [2], Fig. 1.

#### **Results:**

The experimental studies (Fig. 1C and 2A) reveal that freshly embedded brain sections show diattenuation of both types D+ (green) and D- (magenta). With increasing time after embedding the brain sections, the fraction of D- regions decreases (see Fig. 2A). Regions with flat fibers ( $\alpha \approx 5^{\circ}$ , cyan circles) show diattenuation of type D-, regions with intermediate fiber inclinations ( $\alpha \approx 40^{\circ}$ , yellow circles) show both D+ and D-, while regions with steep fibers ( $\alpha \approx 75^{\circ}$ , red circles) only show D+.

The simulations explain this behavior (see Fig. 2B): Diattenuation caused by anisotropic scattering is negative (D-) for flat fibers and positive (D+) for steep fibers (brown triangles); the effect vanishes with increasing embedding time (blue triangles). Diattenuation caused by anisotropic absorption (dichroism, computed analytically [4]) is positive and decreases with increasing fiber inclination. The simulations of the horizontal fiber bundle (see Fig. 1C) show that the diattenuation depends less on the fiber radius distribution and more on myelin sheath thickness, fiber orientation distribution, and fiber size. Regions with strongly myelinated, relatively straight, small and horizontal fibers are expected to yield the strongest negative diattenuation. This allows for example to distinguish regions with many small fibers from regions with few large fibers which both yield similar birefringence (3D-PLI) signals.



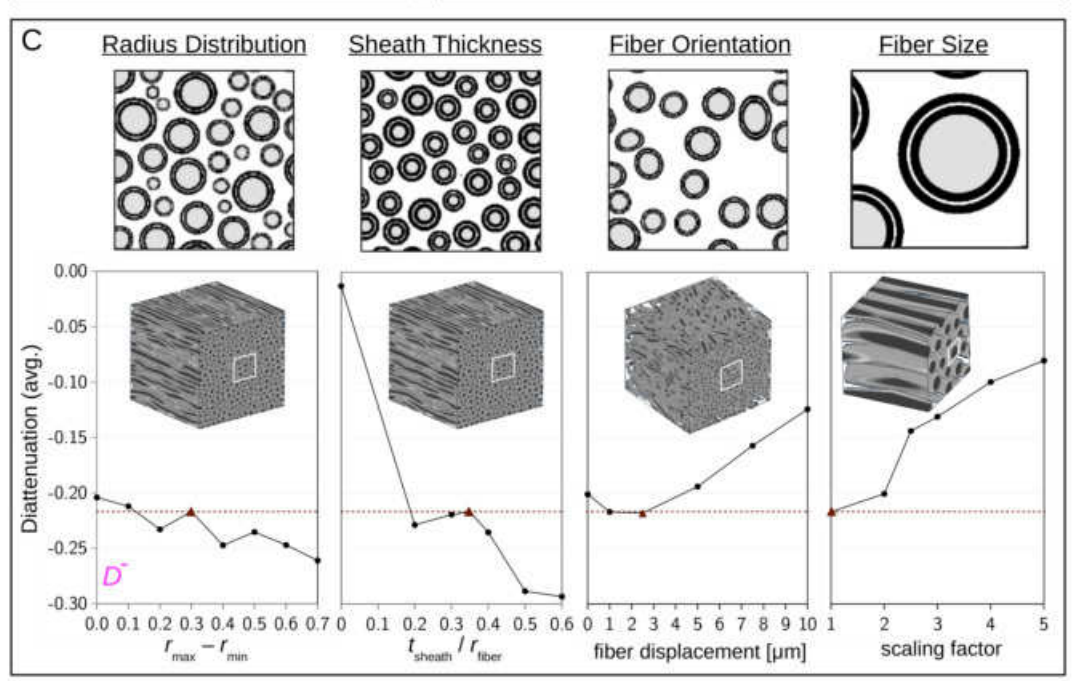


Figure 2. Comparison of measured and simulated diattenuation effects. (A) Diattenuation images of a coronal vervet monkey brain section measured 8 and 51 days after tissue embedding. Diattenuation values that belong to regions with diattenuation of type D+(D-) are shown in green (magenta). The colored circles highlight regions with flat, intermediate, and steep fiber inclinations:  $\alpha=5^\circ$  (cyan),  $\alpha=40^\circ$  (yellow),  $\alpha=75^\circ$  (red). (B) Diattenuation curves (average diattenuation value plotted against the fiber inclination) caused by dichroism (analytical model) and anisotropic scattering (simulated for an artificial fiber bundle). (C) Average diattenuation values of the horizontal fiber bundle simulated for different fiber properties: different fiber radius distributions, myelin sheath thicknesses (relative to the fiber radius), fiber orientation distributions, and fiber sizes. Parts of subfigures A,B have been published in Menzel et al. (2018) [4], Fig. 4.

# **Conclusions:**

Our studies have shown that diattenuation contains additional information about the nerve fiber architecture and tissue composition, which makes Diattenuation Imaging a valuable imaging technique.

# Imaging Methods:

Multi-Modal Imaging Polarized light imaging (PLI) <sup>1</sup>

#### Neuroanatomy:

#### **Keywords:**

Computing

Modeling

Myelin

Neuron

Optical Imaging Systems (OIS)

Structures

White Matter

Other - Nerve Fiber Architecture

## My abstract is being submitted as a Software Demonstration.

No

Please indicate below if your study was a "resting state" or "task-activation" study.

Other

Healthy subjects only or patients (note that patient studies may also involve healthy subjects):

Healthy subjects

Was any human subjects research approved by the relevant Institutional Review Board or ethics panel? NOTE: Any human subjects studies without IRB approval will be automatically rejected.

Not applicable

Was any animal research approved by the relevant IACUC or other animal research panel? NOTE: Any animal studies without IACUC approval will be automatically rejected.

Yes

#### Please indicate which methods were used in your research:

Optical Imaging
Postmortem anatomy
Computational modeling
Other, Please specify - Polarized Light Imaging

## Provide references using author date format

[1] Axer, M. et al. (2011), 'A novel approach to the human connectome: Ultra-high resolution mapping of fiber tracts in the brain', NeuroImage, vol. 54, no. 2, pp. 1091-1101.

[2] Axer, M. et al. (2011), 'High-resolution fiber tract reconstruction in the human brain by means of polarized light imaging (3D-PLI)', Frontiers in Neuroinformatics, vol. 5, no. 34.

[3] Menzel, M. et al. (2017), 'Diattenuation of brain tissue and its impact on 3D polarized light imaging', Biomedical Optics Express, vol. 8, no. 7.

[4] Menzel, M. et al. (2018) 'Diattenuation Imaging reveals different brain tissue properties', arXiv:1806.07712v3.

[5] Menzel, M. et al. (2016), 'Finite-Difference Time-Domain Simulation for Three-Dimensional Polarized Light Imaging', Lecture Notes in Computer Science, K. Amunts, L. Grandinetti, T. Lippert, and N. Petkov, eds., vol. 10087, pp. 73-85, Springer.

## Acknowledgments:

This project has received funding from the Helmholtz Association portfolio theme 'Supercomputing and Modeling for the Human Brain', from the European Union's Horizon 2020 Research and Innovation Programme under Grant Agreement No. 720270 (HBP SGA1) and 785907 (HBP SGA2), and from the National Institutes of Health under grant agreements No. R01MH092311 and 5P40OD010965. We gratefully acknowledge the computing time granted through JARA-HPC on the supercomputer JURECA and JUQUEEN at Forschungszentrum Jülich (FZJ). We thank our colleagues from the Institute of Neuroscience and Medicine (INM-1), FZJ: Markus Cremer, Christian Rademacher, and Patrick Nysten for the preparation of

<sup>&</sup>lt;sup>1|2</sup>Indicates the priority used for review

OHBM 09.12.2019, 10:39 https://ww5.aievolution.com/hb... the histological brain sections, Julia Reckfort, Hasan Köse, David Gräßel, Isabelle Mafoppa Fomat, and Philipp Schlömer for the

the histological brain sections, Julia Reckfort, Hasan Köse, David Gräßel, Isabelle Mafoppa Fomat, and Philipp Schlömer for the polarimetric measurements, and Felix Matuschke for providing the algorithm to generate the fiber configurations. Furthermore, we thank Karl Zilles (INM-1) and Roger Woods (UCLA Brain Mapping Center, Los Angeles) for collaboration in the vervet brain project.